ELSEVIER

Journal of Nuclear Materials 301 (2002) 35–39

journal of nuclear materials

www.elsevier.com/locate/jnucmat

Corrosion and deposition of ferrous alloys in molten lead–bismuth

Ph. Deloffre *, A. Terlain, F. Barbier

DEN/DPC/SCCME/LECNA, CEA-Saclay, 91191 Gif sur Yvette cedex, France

Abstract

This paper reports corrosion and deposition data from tests carried out with liquid eutectic lead–bismuth (Pb–55 at.% Bi) filled steel tubes (austenitic and martensitic) under a thermal gradient (500–280 °C) for 3000 h. For the austenitic steel, the surface exposed to Pb–55Bi exhibited a ferritic corrosion layer depleted in nickel and chromium at temperature above 450 °C. In the temperature range 450–360 °C, deposits composed of iron and chromium were found. There is a temperature effect on composition with a change from iron-rich to chromium-rich with decreasing temperature. For the martensitic steel, a corrosion without corrosion layer was observed above 480 °C. Only one type of deposit consisting of 98Fe–2Cr was found in the 400–480 °C temperature range.

1. Introduction

Liquid eutectic lead–bismuth (Pb–55 at.% Bi) is a candidate material for spallation neutron target and nuclear coolant in accelerator driven systems proposed for radioactive waste transmutation [1]. The advantages of this alloy for these applications are a high atomic number, low melting point, high thermal conductivity, low vapor pressure and no violent reaction with air and water. However, the structural container is exposed to a significant flux of high-energy protons and neutrons as well as a very corrosive environment. It is recognized that steels are severely corroded by liquid lead alloys at high temperature [2–5]. Thus the container material must have a good compatibility with the liquid metal target.

This paper is focused on the corrosion of the containment materials by the Pb–Bi eutectic liquid target. Corrosion by liquid metals can manifest itself in various ways: dissolution, chemical reaction at the solid–liquid interface, liquid penetration at grain boundaries, ... In the case of the Pb–55Bi alloy, the steel corrosion process depends strongly on the oxygen content in the liquid. From the Ellingham diagram, it can be seen that lead and bismuth oxides are less stable than iron oxides. Therefore, in a given temperature range, for some oxygen concentrations, the surface of the steel exposed to Pb–Bi can be oxidized, which protects it from the dissolution [6].

Investigations on corrosion in Pb–55Bi are being carried out and the most relevant parameters such as the alloy velocity, the composition of the liquid (oxygen content, spallation elements generated during the irradiation), the composition of the steel, the temperature gradient... are considered. Recently, corrosion tests of austenitic and martensitic steels were performed in a liquid metal loop under continuous control of the oxygen concentration [7]. This study did not show any corrosion by direct dissolution in the temperature range 470–300 °C and in the presence of Pb–55Bi alloy containing 10^{-6} wt% of oxygen. The absence of dissolution is due to the formation of a protective oxide film on the steel surface.

The oxygen content in Pb–55Bi must be controlled in order to avoid significant dissolution of the material and then release of elements in the melt. In particular, the rates of dissolution have to be known. Simultaneously,

* Corresponding author. Tel.: +33-1 69 08 16 14; fax: +33-1 69 08 15 86.

E-mail address: philippe.deloffre@cea.fr (Ph. Deloffre).

0022-3115/02/$ - see front matter
PII: S0022-3115(01)00724-3

the deposition of the corrosion products resulting from dissolution must be investigated. Deposition constitutes a serious concern with all liquid metals under non-isothermal conditions (thermal gradient increases the amount of dissolution and the accumulation of deposits can lead to plugging [8,9]).

In this paper, we report a study of corrosion and deposition for austenitic and martensitic steels exposed to Pb–55Bi under a temperature gradient. It describes the corrosion behavior and the nature of deposits, and briefly compares the results with what is known in the liquid eutectic lead–lithium environment.

2. Experimental

2.1. Materials and tests

The tested materials were an austenitic stainless steel (type 316L: 67.8Fe–16.83Cr–11.03Ni–2.1Mo–1.54Mn–0.48Si wt%) and a martensitic steel (type 56T5: 86.49Fe–10.51Cr–0.66Ni–0.65Mo–0.61Mn–0.48Nb–0.22Si–0.20C–0.18V wt%). They were used as tubes (internal diameter: 18 mm, length: 300 mm) that were closed at one end by welding and as small plates (corrosion specimens $15 \times 9 \times 1.5$ mm^3). The specimens were used as received after machining (surface roughness: 0.55 μm). After melting of the Pb–55Bi alloy (55.2Bi–44.8Pb wt%) under an argon atmosphere to prevent air contamination, the liquid was maintained at 170–180 °C for 4 h and the oxides formed at the free surface were mechanically removed. At 170–180 °C the oxygen solubility in Pb–55Bi is $C_{O_2} \approx 5 \times 10^{-7}$ wt% [10]. Then, the tubes were filled (Pb–55Bi amount ≈ 550 g) and the specimens were introduced as shown in Fig. 1. Finally, the open end of each tube was sealed under vacuum by electron beam.

The tubes containing the Pb–55Bi alloy and the corrosion specimens were placed vertically in a furnace under a temperature gradient. The gradient was such that the hot zone of the tube was at the top in order to minimize thermal convection. The temperature was measured each centimeter along the tubes, using thermocouples located in fingers placed near the external surface of the tube.

The hot zone (corrosion area) was about 5 cm high whereas the temperature variation in non-isothermal zone was about 10 °C per cm, leading to a temperature gradient of 220 °C. The test durations were 3000 h. At the test completion, the heating was stopped and the tubes were cooled in ambient air.

2.2. Characterization techniques

After the tests, the tubes were opened in a glove box and then heated in order to empty them and to recover the plates. Then they were cut longitudinally. Before weight measurements, one quarter of the tube and the plates were dipped in a chemical mixture (1/3 ethanol, 1/3 acetic acid, 1/3 hydrogen peroxide) to remove the residual Pb–55Bi alloy adhering to the surface. Then specimens and tubes were cut perpendicularly in several pieces which were polished. In this manner, the steel/Pb–55Bi interface was available for observation. The walls of tubes as 5 cm long pieces (direct view) and the polished samples (cross-section) were observed by optical microscopy, scanning electron microscopy (SEM) and analyzed by microprobe.

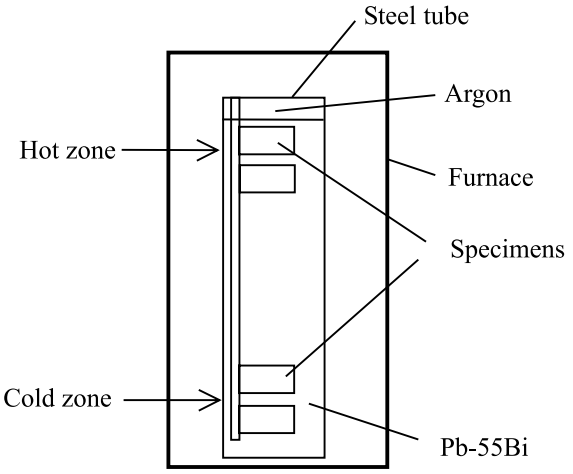

Fig. 1. Schematic drawing of the steel tube and plates exposed to Pb–55Bi.

3. Results and discussion

3.1. Austenitic steel 316L

The surface of the austenitic steel 316L exposed to Pb–55Bi locally exhibited a 10–35 μm thick porous ferritic corrosion layer at temperatures above 450 °C (Figs. 2 and 3). The corroded zones represented only 1/10th of the tube and specimens surface (Fig. 2(a)). The non uniformity of the attack probably results from the initial oxide layer at the steel surface (unwetted zones) [5]. SEM and microprobe analysis of the corrosion layer show that it mainly consists of Fe, almost completely depleted in nickel (0.2 wt%) and severely depleted in chromium (1 wt%) [11]. No noticeable change of molybdenum, manganese and silicium concentrations are observed [11]. The corrosion layer was filled with Pb–55Bi and the boundary between the ferritic layer and the unattacked austenite was well defined with no intermediate apparent diffusion layer. The same behavior with a corrosion on all the specimens surface was obtained in isothermal liquid static Pb–55Bi with oxygen concen-

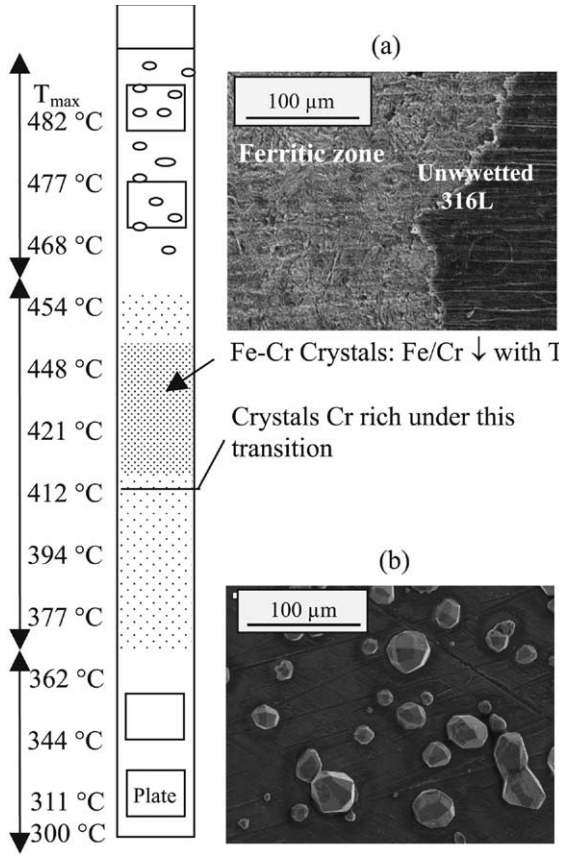

Fig. 2. Behavior of the austenitic steel 316L plates and the tube in contact with Pb–Bi liquid under a thermal gradient. $t = 3000$ h, $C_{O_2} \approx 5 \times 10^{-7}$ wt%. (a) SEM micrograph showing a surface direct view of the tube (ferritic zone $\approx 1/10$th of the wall) and (b) SEM mircrograph showing Fe–Cr crystals.

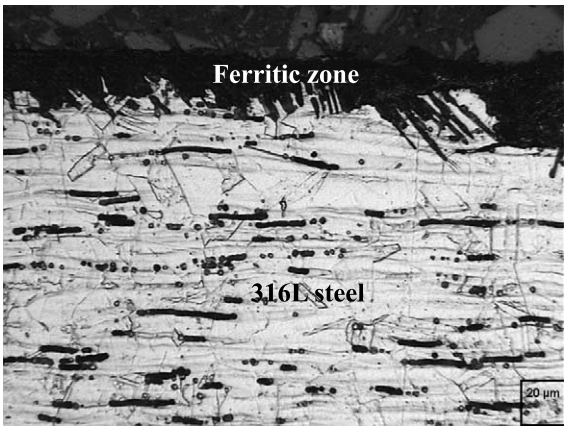

Fig. 3. Cross-section micrograph of austenitic steel 316L after exposure to Pb–Bi at 450 °C for 3000 h, $C_{O_2} \approx 5 \times 10^{-7}$ wt%.

tration of 7×10^{-8} wt% at $T = 500$ °C in our COLIMESTA device [11]. In this later case, the corrosion rate was 230 μm year^{-1} by taking into account the ferritic layer and assuming a linear kinetics. These corrosion mechanism and magnitude of attack are similar to that obtained with the dynamic liquid alloy Pb–17Li at this temperature [3–5]. At $T \approx 475$ °C, the corrosion rate was about 90–180 μm year^{-1} in semi-stagnant Pb–17Li [3–5]. In the two cases, it can be explained by a preferential dissolution of Ni in the liquid due to its high solubility, when no oxide layer is present to protect the surface.

The existence of a dissolution in the hot part of the tube implies mass transfers of the elements dissolved towards the coldest parts.

In the temperature range 360–450 °C, many crystals were observed adhering to the wall of the tube and in frozen alloy (Fig. 2). They were very numerous between 410 and 450 °C. Their average composition was 90Fe–10Cr at about 440 °C and 80Cr–20Fe at about 350 °C with the same morphology. Therefore, there is a temperature effect on the composition: it changes from iron-rich to chromium-rich with decreasing temperature. The Fe/Cr ratio of these crystals decreases continuously with the temperature. The other elements present in austenitic steel 316L in particular Ni are not detected in the crystals. The composition of these crystals results from to the low solubility of iron and chromium in Pb–55Bi, compared to the high solubility of nickel [10]. In this respect, the analyses of Pb–55Bi after treatment give 11 ppm of Ni compared to 1 ppm before test. The quantity of Ni found in the Pb–55Bi after tests was in agreement with that estimated from to the ferritic corrosion layer thickness free from nickel.

Finally, in the range of temperatures lower than to 360 °C no deposit is observed.

These observations are in agreement with those reported in literature and obtained with Pb–17Li liquid alloy [9]. In that case, in regions at temperature ranging from 500 to 400 °C deposits mainly composed of iron and chromium (87Fe–11Cr–1Ni–1Mn) were observed in the hot zone. In addition, for temperatures around 480 °C, crystals of composition 56Fe–44Cr were also detected and in the temperature range 480–450 °C Cr-rich crystals (70Cr–30Fe) were observed. The presence of Ni and Mn in crystals comes from their lower limit of solubility in Pb–17Li than in Pb–55Bi. It also explains that at temperatures lower than 370 °C the presence of crystals (36–40)Ni–(25–18)Mn–(35–46)Sn is not found in the case of Pb–55Bi.

3.2. Martensitic steel 56T5

In contrast with austenitic 316L steel, the corrosion morphology of 56T5 martensitic steel is characterized by an homogeneous dissolution without formation of a superficial corrosion layer (Figs. 4 and 5). This dissolution

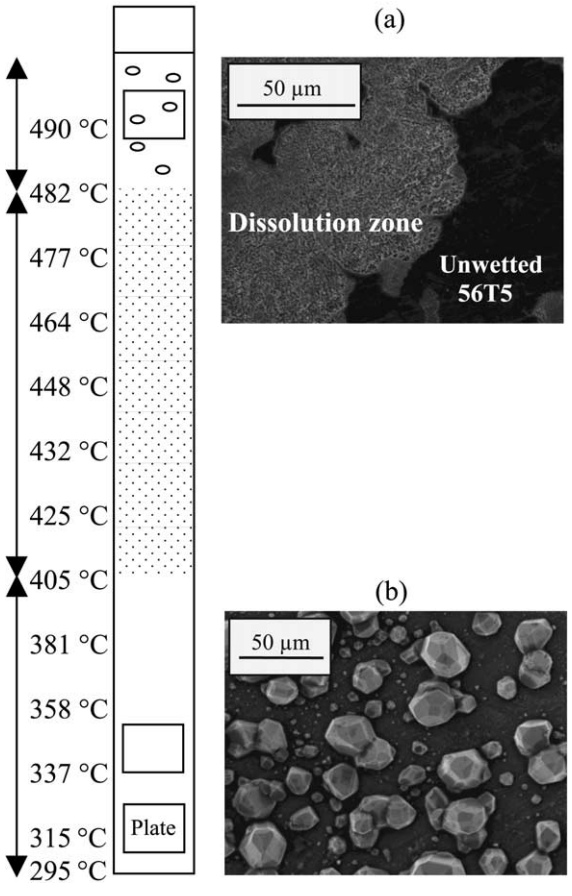

Fig. 4. Behavior of the plates and the tube martensitic steel 56T5 in contact with Pb–Bi liquid under a thermal gradient. $t = 3000$ h, $C_{O_2} \approx 5 \times 10^{-7}$ wt%. (a) SEM micrograph showing a surface direct view of the tube (dissolution zone $\approx 1/50^{eme}$ of the wall) and (b) SEM mircrograph showing 98Fe–2Cr crystals.

occurs at temperatures above 480 °C and dissolution zones are not uniform and represented only 1/50th of the tube and specimens surface (Fig. 4(a)). For this reason, it was not possible to determine the specimens loss of weight. However, an increase in the surface roughness was observed but microprobe analysis did not show any chromium or iron depletion near the interface [11]. The main constituents of this steel seem to dissolve at a similar rate in molten Pb–55Bi, but cross-section micrograph reveals an 10–20 μm intergranular attack (Fig. 5). The same behavior with a corrosion on all the specimens surface was obtained in isothermal liquid static Pb–Bi with oxygen concentration of 7×10^{-8} wt% at $T = 500$ °C in our COLIMESTA device [11]. In that case, assuming a linear kinetics, the dissolution rate was 45 μm year^{-1}. This intergranular attack of the martensitic steels by Pb–55Bi was also observed by Cliffort for temperatures above 700 °C [12]. A dissolution of the

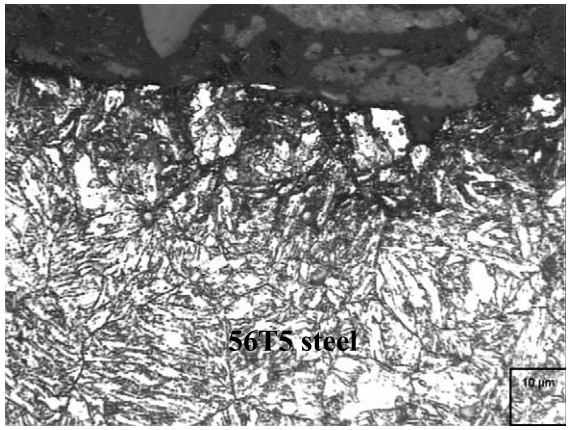

Fig. 5. Cross-section micrograph of martensitic steel 56T5 after exposure to Pb–Bi at 480 °C for 3000 h, $C_{O_2} \approx 5 \times 10^{-7}$ wt%.

martensitic steels was also seen in the dynamic ($v \geqslant 1.9$ cm s^{-1}) liquid alloy Pb–17Li at 500 °C, but in that case no intergranular attack was found [3–5]. The existence of a dissolution in the hot part of the tube implies mass transfers of the elements dissolved towards the coldest parts.

In the 400–480 °C temperature range, the deposition of corrosion product takes place in a uniform way on the whole of the tube surface. The deposits consist of crystals very rich in iron (98Fe–2Cr). The composition is independent of the temperature. The other elements present in martensitic steel 56T5 are not detected in the crystals. The composition of these crystals may be attributed to the low solubility of iron and chromium in Pb–55Bi [10].

Finally, at temperatures lower than 400 °C no deposit is observed. These observations are different from those reported in literature obtained with Pb–17Li liquid alloy [9]. In that case, different types of crystals were detected, composed of Fe and Cr or a mixture of Fe, Cr, Ni, and Mn with Fe/Cr ratio decreasing with the temperature. The deposition process difference in Pb–55Bi and Pb–17Li can be attributed to the solubility difference of the metallic elements in Pb–55Bi [12] and Pb–17Li.

4. Conclusions

A series of deposition tests have been carried out in liquid Pb–55Bi containing austenitic 316L and martensitic 56T5 steel tubes under thermal gradients and oxygen concentrations of around 5×10^{-7} wt%.

In the hot zone ($T > 450$ °C), the 316L specimen surface is covered by a porous ferritic corrosion layer. At temperatures below 360 °C deposits composed of iron and chromium were found. They were Fe rich at the highest temperatures and Cr rich at the lowest temper-

atures. The Fe/Cr ratio of these crystals continuously decreases with the temperature. At temperatures lower than 360 °C no deposit is observed.

For the martensitic steel 56T5, above 480 °C, the corrosion is characterized by a homogeneous dissolution without the formation of a superficial corrosion layer but with an intergranular attack. In the range of temperature 400 and 480 °C, the deposits of corrosion products were composed of iron-rich crystals (98Fe–2Cr). Their composition is independent of the temperature. In the range of temperatures lower than 400 °C no deposition was observed.

Thus, at $T \approx 500$ °C the austenitic and martensitic steels are corroding in eutectic Pb–55Bi under a thermal gradient (500–280 °C), because no protecting oxide layer is formed if the oxygen content is kept at around 5×10^{-7} wt%.

References

[1] M. Salvatores, I. Slessarev, A. Zaetta, M. Delpech, G. Ritter, R. Soule, M. Vanier, CEA report, NT-DRN-98-001, Commissariat à l'Energie Atomique, 1998.

[2] M. Broc, J. Sannier, G. Santarini, Behaviour of ferritic steels in the presence of flowing purified liquid lead, in: Proceedings of the BNES international conference: Liquid Metal Engineering and Technology, BNES, London, 1984, p. 361.

[3] J. Sannier, T. Flament, A. Terlain, Fusion Technol. 1 (1991) 901.

[4] J. Sannier, M. Broc, T. Flament, A. Terlain, Fusion Eng. Design 14 (1991) 299.

[5] T. Flament, P. Tortorelli, V. Coen, H.U. Borgstedt, J. Nucl. Mater. 191–194 (1992) 132.

[6] V. Markov, Seminar on the Concept of Lead–Cooled Fast Reactors, 22–23 September, 1997, Cadarache, France, private communication.

[7] F. Barbier, A. Rusanov, J. Nucl. Mater. 296 (2001) 231.

[8] P.F. Tortorelli, Fus. Eng. Des. 14 (1991) 335.

[9] F. Barbier, J. Nucl. Mater. 283–287 (2000) 1267.

[10] Y.I. Orlov, A.D. Efanov, V.M. Troyanov, Performance of works under contrat No 501068B049630 between SSC RF IPPE and Research Center Cadarache, Report substage 2.1, IPPE/Obninsk, 1998.

[11] Ph. Deloffre, F. Barbier, C. Delisle, C. Blanc, CEA report, RT-SCECF 555, Commissariat à l'Energie Atomique, 2000.

[12] J.C. Clifford, G. Burnet, Chem. Eng. Prog. 67–73 (1962) 58.